sustainability

MDPI

Article

Air Quality Changes during the COVID-19 Lockdown in an Industrial City in North China: Post-Pandemic Proposals for Air Quality Improvement

Hongya Niu [1], Chongchong Zhang [1], Wei Hu [2,*], Tafeng Hu [3], Chunmiao Wu [1], Sihao Hu [1], Luis F. O. Silva [4], Nana Gao [1], Xiaolei Bao [5] and Jingsen Fan [1]

[1] School of Earth Sciences and Engineering, Hebei University of Engineering, Handan 056038, China
[2] Institute of Surface-Earth System Science, School of Earth System Science, Tianjin University, Tianjin 300072, China
[3] Institute of Earth Environment, Chinese Academy of Sciences, Xi'an 710061, China
[4] Department of Civil and Environmental, Universidad de la Costa, Calle 58 #55-66, Barranquilla 080002, Atlántico, Colombia
[5] Hebei Chemical & Pharmaceutical College, Shijiazhuang 050026, China
* Correspondence: huwei@tju.edu.cn

Abstract: To better understand the changes in air pollutants in an industrial city, Handan, North China, during the COVID-19 lockdown period, the air quality and meteorological conditions were recorded from 1 January to 3 March 2020 and the corresponding period in 2019. Compared to the corresponding period in 2019, the largest reduction in $PM_{2.5–10}$, $PM_{2.5}$, NO_2 and CO occurred during the COVID-19 lockdown period. $PM_{2.5–10}$ displayed the highest reduction (66.6%), followed by NO_2 (58.4%) and $PM_{2.5}$ (50.1%), while O_3 increased by 13.9%. Similarly, compared with the pre-COVID-19 period, NO_2 significantly decreased by 66.1% during the COVID-19 lockdown, followed by $PM_{2.5–10}$ (45.9%) and $PM_{2.5}$ (42.4%), while O_3 increased significantly (126%). Among the different functional areas, $PM_{2.5}$ and $PM_{2.5–10}$ dropped the most in the commercial area during the COVID-19 lockdown. NO_2 and SO_2 decreased the most in the traffic and residential areas, respectively, while NO_2 increased only in the township and SO_2 increased the most in the industrial area. O_3 increased in all functional areas to different extents. Potential source contribution function analysis indicated that not only the local air pollution lessened, but also long-distance or inter-regional transport contributed much less to heavy pollution during the lockdown period. These results indicate that the COVID-19 lockdown measures led to significantly reduced PM and NO_2 but increased O_3, highlighting the importance of the synergetic control of $PM_{2.5}$ and O_3, as well as regional joint prevention and the control of air pollution. Moreover, it is necessary to formulate air pollution control measures according to functional areas on a city scale.

Keywords: COVID-19 lockdown; industrial city; air quality; potential source contribution function

Citation: Niu, H.; Zhang, C.; Hu, W.; Hu, T.; Wu, C.; Hu, S.; Silva, L.F.O.; Gao, N.; Bao, X.; Fan, J. Air Quality Changes during the COVID-19 Lockdown in an Industrial City in North China: Post-Pandemic Proposals for Air Quality Improvement. *Sustainability* **2022**, *14*, 11531. https://doi.org/10.3390/su141811531

Academic Editor: Yichen Wang

Received: 3 July 2022
Accepted: 6 September 2022
Published: 14 September 2022

1. Introduction

Air pollution is a public environmental issue in some regions across the world, and $PM_{2.5}$ exposure contributed to 4.58 million deaths and 142.52 million disability-adjusted life years globally in 2017 [1]. In China, there were 1.42 and 0.93 million deaths attributable to $PM_{2.5}$ and O_3 exposure in 2019, respectively (https://www.stateofglobalair.org/health/pm (accessed on 5 September 2022)). In order to improve air quality and habitable environments, the Chinese government has released a series of policies, such as the "Air Pollution Prevention and Control Action Plan" in 2013 [2]. As a result, the concentration of $PM_{2.5}$ in the Beijing-Tianjin-Hebei (BTH) region decreased by 25% from 2013 to 2017 [3]. The coal substitution policy (i.e., "coal-to-gas" and "coal-to-electricity") has been implemented in northern China step by step since 2010s. In 2018, the Chinese government issued "Opinions

on Comprehensively Strengthening Ecological Environmental Protection and Resolutely Fighting the Tough Battle of Pollution Prevention and Control", which focused on industries such as iron and steel, coking, and benchmarked them against world-class standards, formulated and implemented local standards for the ultra-low emissions of air pollutants.

With the implementation of these policies, changes in energy structure are necessary for improving air quality [4]. For instance, Handan, an industrial city, as one of the "2 + 26" cities with severe air pollution in Hebei province, has significantly improved its air quality [5,6]. The annual average concentrations of PM_{10}, $PM_{2.5}$, SO_2, NO_2 and CO in Handan decreased from 153 μg/m^3, 85 μg/m^3, 36 μg/m^3, 50 μg/m^3 and 3.4 mg/m^3 in 2017 to 124 μg/m^3, 66 μg/m^3, 15 μg/m^3, 38 μg/m^3 and 2.6 mg/m^3 in 2019, respectively, while the annual average concentration of O_3-8h (the eight-hour average ozone concentration) remained at a high level with concentrations of 195 and 201 μg/m^3 in 2017 and 2019. Although air pollution was generally alleviated, the levels of air pollutants remain dangerously high and largely exceed the World Health Organization (WHO) air quality guideline values (https://www.who.int/news-room/fact-sheets/detail/ambient-(outdoor)-air-quality-and-health (accessed on 5 September 2022)). The hourly and daily concentrations of air pollutants also frequently surpass the National Ambient Air Quality Standard (GB 3095-2012). Therefore, far greater effort should be made to improve air quality in Handan and other similar cities.

In January 2020, the COVID-19 broke out in China and across the world. In order to control the spread of the COVID-19, the Chinese government launched a Level 1 Public Health Emergency Response and implemented a series of lockdown measures [7,8]. In the short term, typical anthropogenic emission sources such as vehicle exhausts, cooking, construction and industries largely decreased, leading to the decrease in air pollutants [9,10]. This special period offered a rare and valuable opportunity to more accurately study how the reduction in local emissions influenced air quality in typical industrial cities in northern China [11–13] and provided a background reference for studying regional air pollution in normal periods. Therefore, it is of great significance to study air quality during the COVID-19 period for the formulation and implementation of air pollution control measures.

A large number of studies examined air quality changes in cities during the COVID-19 lockdown both within and across countries, as reviewed previously [14]. For instance, in India, which is the county ranked second among 15 countries for premature deaths related to outdoor air pollution in 2010, following China [15], during the COVID-19 period, PM_{10}, $PM_{2.5}$, NO_2 and SO_2 concentrations were reduced by 55%, 49%, 60% and 19%, respectively, in Delhi, and by 44%, 37%, 78% and 39%, respectively, in Mumbai in the Indo-Gangetic Plain [16]. It was reported that NO_2 and PM_{10} declined, respectively, by 44.0% and 40.3% in an urban-industrial area of mainland Portugal during the national lockdown from March to May 2020 [17]. However, other studies found that the increases in the concentrations of O_3 (by 7 to 7.4 μg/m^3 or 14 to 17% at urban stations) were broadly in line with NO_2 reductions, and increases in both PM_{10} (5.9 to 6.3 μg/m^3) and $PM_{2.5}$ (3.9 to 5.0 μg/m^3) were recorded at both rural and urban stations in the United Kingdom during the lockdown [18]. Another global study of eight cities reported significant nonlinear relationships between the COVID-19 lockdown and air pollution, and variations in the magnitude of changes in pollutant levels due to local conditions [19]. Therefore, it has been suggested that, due to the complexity of the atmospheric system, more studies should be performed to better understand the roles of atmospheric compositions, meteorological conditions and emissions from specific sectors [20,21], such as different functional areas, to be able to make effective policies based on the reductions caused by the COVID-19 lockdown.

Some studies have reported the effect of the lockdown measures during the COVID-19 period on air quality in China. These studies can be classified into three groups. Firstly, some studies focused on individual cities. For example, Lian et al. [22] demonstrated that the lockdown reduced the concentrations of $PM_{2.5}$, PM_{10}, SO_2, NO_2 and CO by 3.9–53.3% (except O_3) in Wuhan, and Hu et al. [23] showed that the emissions of SO_2, NO_x, $PM_{2.5}$ and volatile organic compounds (VOCs) decreased by 11–47% in Shanghai, respectively, com-

pared with those during the pre-Chinese New Year period. Secondly, some studies selected neighboring cities or regions for comparison. For instance, Zhang et al. [24] showed that compared with the pre-COVID-19 period, the concentrations of $PM_{2.5}$, PM_{10}, SO_2, NO_2 and CO were lowered by 37%, 30%, 29%, 52% and 33% in the Guanzhong Basin of northwest China, but O_3 concentration substantially increased. Wang et al. [25] divided 358 Chinese cities into eight climatic regions and found that $PM_{2.5}$ decreased by 59.0–64.2% in cold regions (northeastern and northwestern China), while O_3 soared by 99.0–99.9% in warm regions (central south and southern coastal China); climate had less influence on NO_2, which decreased by 41.2–57.1% countrywide during the lockdown. Finally, some studies selected several megacities for comparison. For example, Pei et al. [26] found that NO_2 plunged across Beijing, Wuhan and Guangzhou, while $PM_{2.5}$, SO_2 and HCHO (as a proxy to VOCs) remained stable in major cities during the COVID-19 lockdown. Wang et al. [8] estimated that the lockdown reduced ambient NO_2 concentrations by 36–53% in six megacities (Beijing, Chengdu, Shenzhen, Xi'an, Shanghai and Wuhan) in China. However, studies on the variations of air pollutants among different functional areas and in industrial areas during the COVID-19 lockdown have been rare, thus, there is a lack of direct understanding of the effect of the COVID-19 lockdown on emission changes.

In this study, we analyzed air quality and meteorological conditions before and after COVID-19 (during 1 January to 3 March 2020) in an industrial city, Handan, in northern China, and compared the observed results with the corresponding period in 2019. Furthermore, we compared the differences in air quality changes at nine different functional areas, including traffic area, industrial area, commercial area, construction site, residential area, township area, enterprise area, scenic area and village. Moreover, correlation analysis and potential source contribution function (PSCF) analysis were used to explore the possible factors resulting in air quality changes in Handan city during the COVID-19 period, which will provide scientific support to formulate air pollution control policies and improve air quality in China.

2. Methodology

2.1. Study Area

Handan, with a population of 9.55 million, is a city known as a key old industrial base in North China. Handan is bordered by the Taihang Mountains to the west and the North China Plain to the east and belongs to China's Third Ladder; the terrain is high in the west and low in the east, which is not conducive to the diffusion of air pollutants (Figure 1). Moreover, Handan is located at the junction of the four major provinces (Hebei, Henan, Shandong, and Shanxi) with intense pollutant emissions in China, and the air pollution is serious [27]. Hence, it is easy to increase the interregional transport of air pollutants. It has been reported that Handan was one of the five cities with the worst air quality among 338 cities in China in the past five years.

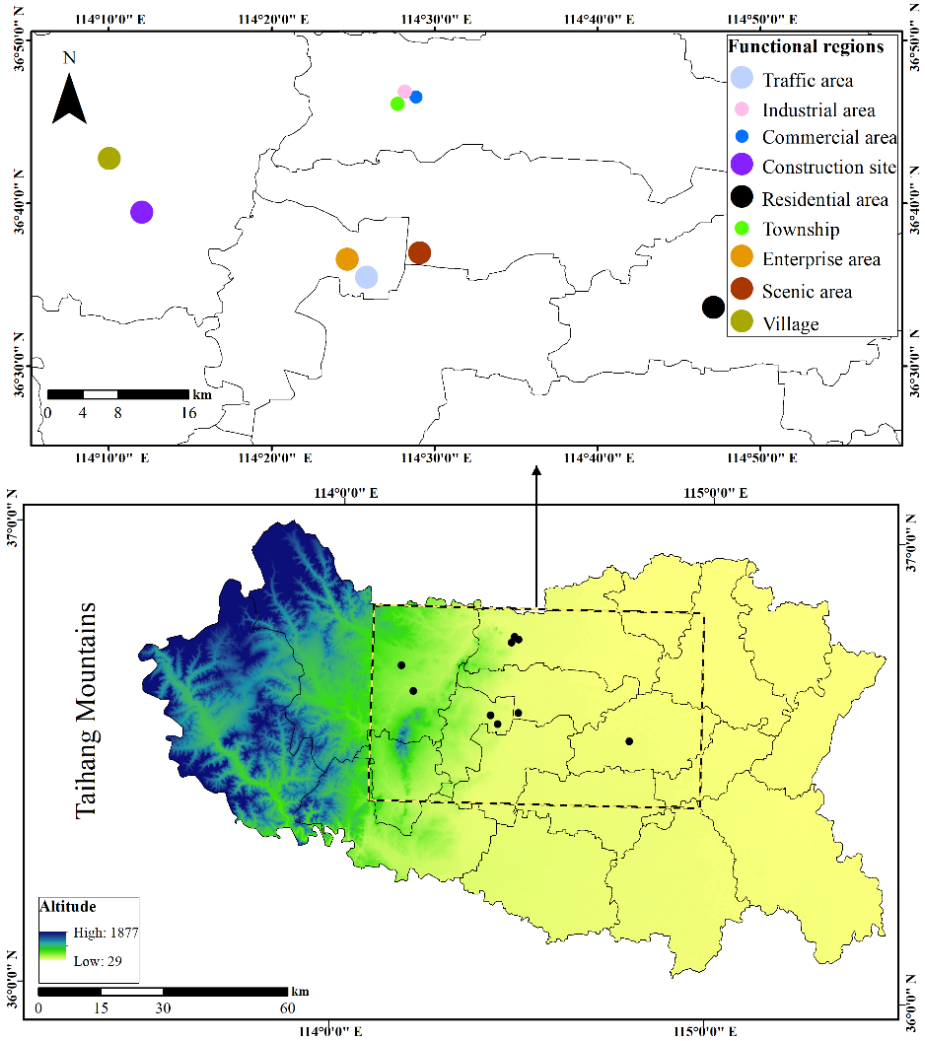

Figure 1. Locations of the observation sites at nine functional areas in Handan.

2.2. Observation and Data Sources

In order to study the changes in air quality in Handan city during the COVID-19 period, the daily air quality data (i.e., air quality index (AQI), PM_{10}, $PM_{2.5}$, NO_2, SO_2, CO and O_3) of Handan measured during the COVID-19 period (from 1 January to 3 March) in 2020 and the corresponding period (13 January to 16 March) in 2019 were obtained from the Grid Precision Monitoring and Decision Platform (http://117.78.34.120:8007/BigData/Main (accessed on 5 September 2022)). The meteorological parameters including temperature, relative humidity (RH) and wind speed during the COVID-19 period in 2020 and the corresponding period in 2019 were also obtained from the same platform. The air quality and meteorological data were the averages of measurement results from national air quality monitoring stations in Handan.

The daily ambient air pollutant concentrations of nine different functional areas in Handan were measured during the COVID-19 period (1 January to 3 March) in 2020, which were conducted by the local monitoring stations at the representative sites (Figure 1). Detailed information about the nine monitoring sites can be found in Table S1.

Based on the National Contingency Plan for Public Health Emergencies issued by the State Council and the epidemic prevention and control situation, Hebei Province launched a Level 1 Public Health Emergency Response on 24 January 2020, which was also the traditional Chinese New Year's Eve. In order to exclude the impact of festival activities during the Chinese New Year period on air quality, the period from 21 January to 31 January was labeled as the Chinese New Year period. Handan resumed essential aspects of

life and production on 14 February 2020, although a large area was still under epidemic prevention and control. According to this timeline, to better understand the changes in air pollutants, the whole observation period (named as the COVID-19 period in this study) was divided into four stages: Stage I: pre-COVID-19 period (1–20 January 2020); Stage II: the Chinese New Year period (21–31 January 2020); Stage III: COVID-19 lockdown period (1–14 February 2020); and Stage IV: post-COVID-19 period (15 February–3 March 2020).

For comparison, the corresponding period from 13 January to 16 March 2019 was chosen based on the date of the Chinese New Year in 2019 (5 February 2019, corresponding to the Chinese New Year on 25 January 2020) and correspondingly divided into four stages. This ensured that the impact of human activities on air pollution during the Chinese New Year period was consistent, and the comparison analysis could be more accurate. Moreover, the relation of meteorological factors with the lunar calendar is better than that with the solar calendar, which can reduce the difference in the impact of meteorological factors on air pollution in different years.

2.3. Backward Trajectory and Potential Source Contribution Function Analysis

Twenty-four-hour backward trajectories of air masses starting from Handan city (36.61° N, 114.19° E, 500 m above ground level) during the COVID-19 period were calculated with MeteoInfo 3.0.4 combined with TrajStat software (http://www.meteothink.org/index.html, accessed on 5 September 2022), and meteorological data were downloaded from the National Center for Environmental Prediction (NCEP) Global Data Assimilation System (GDAS))). The air mass trajectories were clustered into 6 types of trajectories using the Euler method.

Potential source contribution function (PSCF) is a method to preliminarily identify major source regions of air pollutants based on airmass trajectory analysis [28,29]. The area covered by all the airmass trajectories calculated during the observation period was divided into 0.5° × 0.5° grids. Then, the *PSCF* value was calculated as follows:

$$PSCF_{ij} = \frac{M_{ij}}{N_{ij}} \quad (1)$$

where N_{ij} is the number of the trajectory segment endpoints over Grid ij, and M_{ij} is the number of these endpoints with the pollutant concentration higher than a criterion value over Grid ij. The threshold was set as the second-level average daily standard value of 75 μg/m^3 in China's Ambient Air Quality Standard. In order to reduce the uncertainty caused by the small number of N_{ij} in some grids, the weight factor W_{ij} was introduced as Equations (2) and (3). The weighted *PSCF* (*WPSCF*) value is obtained by multiplying *PSCF* value with W_{ij}. The calculation formula is as follows [30,31].

$$WPSCF_{ij} = PSCF_{ij} \times W_{ij} \quad (2)$$

$$W_{ij} = \begin{cases} 1, & 80 < N_{ij} \\ 0.7, & 20 < N_{ij} \leq 80 \\ 0.42, & 10 < N_{ij} \leq 20 \\ 0.05, & N_{ij} \leq 10 \end{cases} \quad (3)$$

3. Results and Discussion

3.1. Variations in Meteorological Conditions and Air Pollutants

3.1.1. Meteorological Conditions

Meteorological conditions play an important role in air pollution [32–34]. Figure 2 shows the time series of hourly meteorological parameters in Handan during the COVID-19 period in 2020 and the corresponding period in 2019. Figure 3 shows the differences in meteorological parameters between 2019 and 2020.

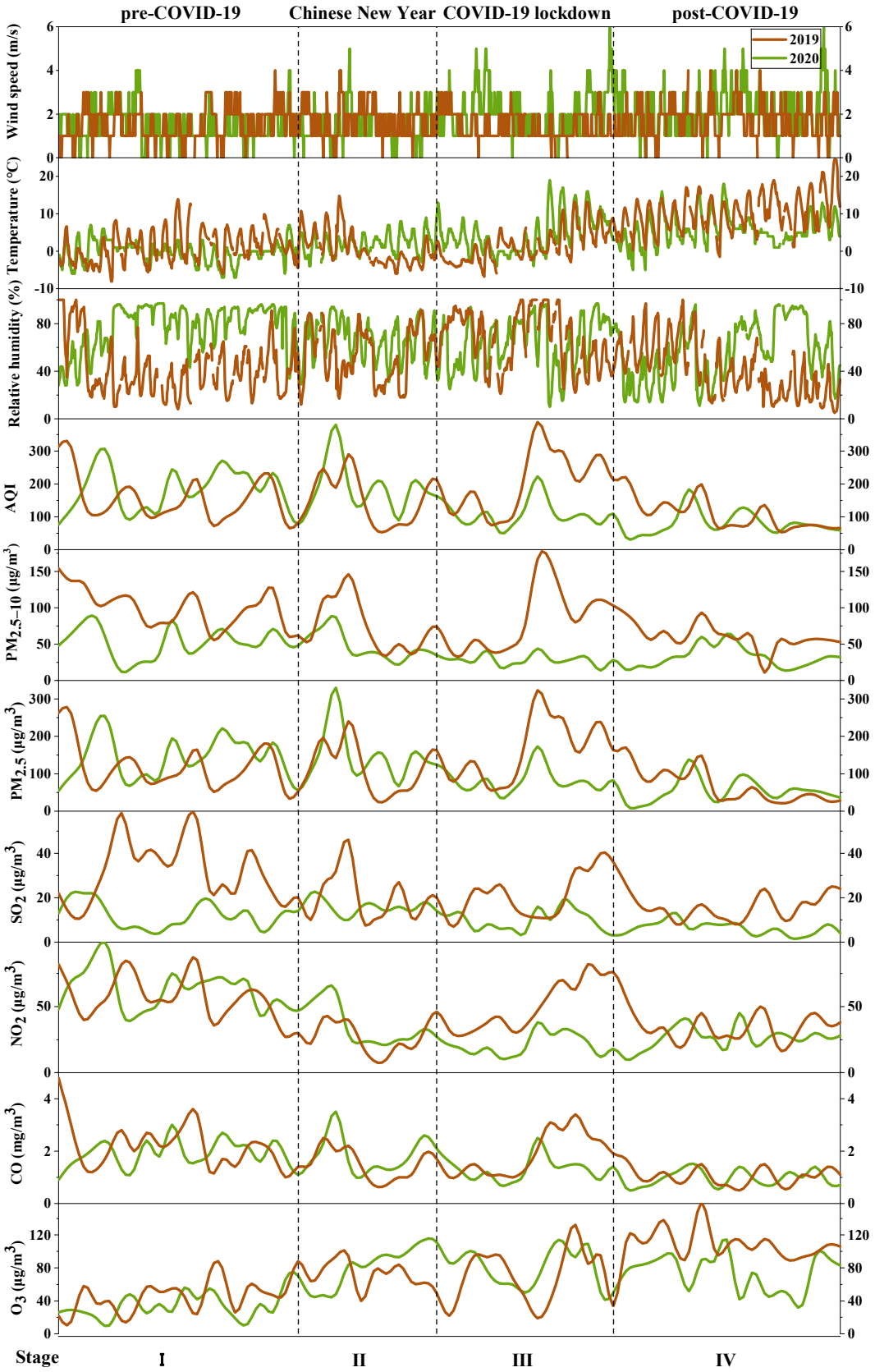

Figure 2. Variations in meteorological parameters (hourly), AQI and air pollutants (daily) in Handan during the COVID-19 period in 2020 and the corresponding period in 2019. $PM_{2.5–10}$ was the coarse fraction of PM_{10} with aerodynamic diameter larger than 2.5 μm, calculated as the difference between PM_{10} and $PM_{2.5}$.

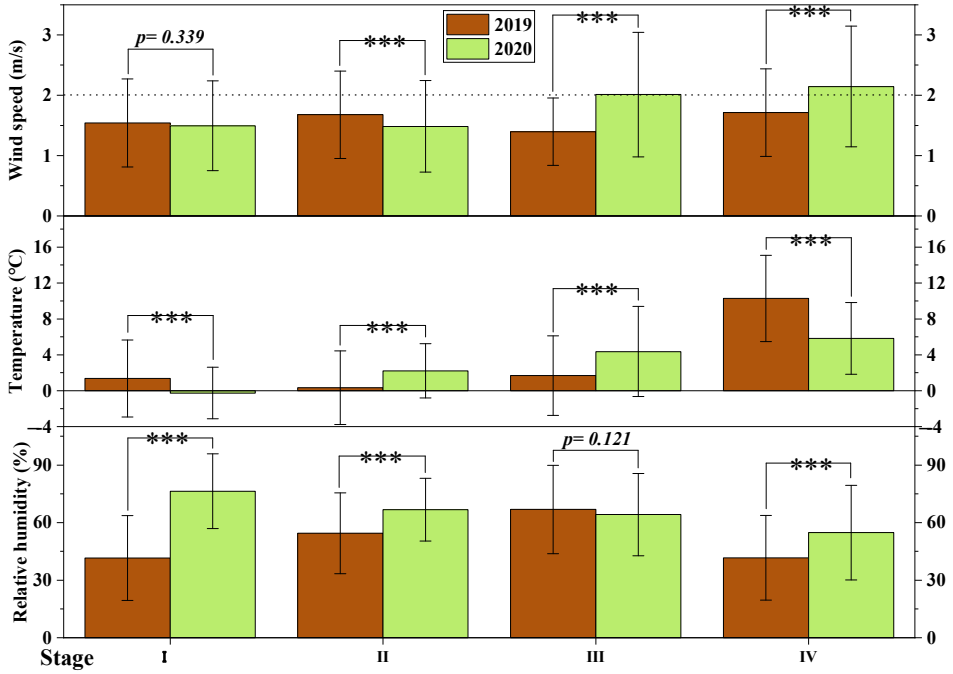

Figure 3. Averages of meteorological parameters in Handan during the COVID-19 period in 2020 and the corresponding period in 2019. The brackets with *** means meteorological parameters have significant differences (independent-samples *t*-test, $p < 0.05$) between 2019 and 2020.

During Stage I (pre-COVID-19), there was no significant difference (*t*-test, $p > 0.05$) in wind speed between 2019 and 2020, while air temperature was lower, and RH was higher in 2020 ($p < 0.05$) (Figure 3). RH is a very important factor to favor hygroscopic growth and secondary formation, which can substantially aggravate particulate pollution in North China during winter [35]. Therefore, during Stage I the meteorological conditions might aggravate the accumulation of air pollutants and secondary formation via aqueous-phase chemical reactions [36]. During Stage III (COVID-19 lockdown), there was no significant difference ($p > 0.05$) in RH between 2019 and 2020. Although there were statistical differences in air temperature and wind speed during Stage III, the air was quite stable with weak wind (average wind speed < 3 m/s, i.e., static weather) and low air temperature (<4 °C), which inhibited the dispersal of the pollutants. Zhang et al. (2019) [37] reported that meteorological conditions had less impact than anthropogenic emissions based on $PM_{2.5}$ trends from 2013 to 2017 in China. Zhang et al. [38] reported that in 2017 relative to 2013, only approximately 13% of the total $PM_{2.5}$ reduction resulted from meteorological changes in the BTH region. Considering the synergistic effects of various meteorological factors, the impacts of meteorological conditions on air quality in 2020 could be regarded as close to that in 2019 during Stage III.

3.1.2. Air Pollutants

According to the air quality during the five years of 2015–2019 in Handan, severe air pollution usually occurs during October to March (next year), and severe pollution days accounted for over 95% of the days in these months every year. The annual mean $PM_{2.5}$ decreased gradually from 96.5 μg/m^3 in 2015 to 71.0 μg/m^3 in 2019 in Handan and the decreasing rate slowed down from 2018 (74.6 μg/m^3) to 2019 (71.0 μg/m^3), similar to the conditions in the BTH region and surrounding areas (the annual decreasing rate was 7.8–11.8% from 2015 to 2018 and 1.7% from 2018 to 2019) (http://117.78.34.120:8007/BigData/Main (accessed on 5 September 2022)). Therefore, given the meteorological conditions and declining trends of air pollutants, the comparison of air pollutants during Stage III between 2020 and 2019 can efficiently reflect the impact of the COVID-19 lockdown on air quality.

Figure 4 shows that short-term control measures due to the COVID-19 lockdown had an obvious effect on reducing air pollutants in the North China Plain. The average $PM_{2.5}$ concentration in 42 cities of the North China Plain was 49 μg/m^3 during the COVID-19 lockdown period, which was dramatically reduced from 117 μg/m^3 (by 58%) during the corresponding period (Stage III) in 2019. This result indicated that the reduction in anthropogenic emissions largely reduced $PM_{2.5}$ pollution in the NCP. Xing et al. [39] estimated the emission changes during the COVID-19 lockdown (23 January–5 March) using a response model and found that the anthropogenic emissions of primary $PM_{2.5}$ on the NCP were reduced by 63% compared to hypothetical emissions without lockdown effects.

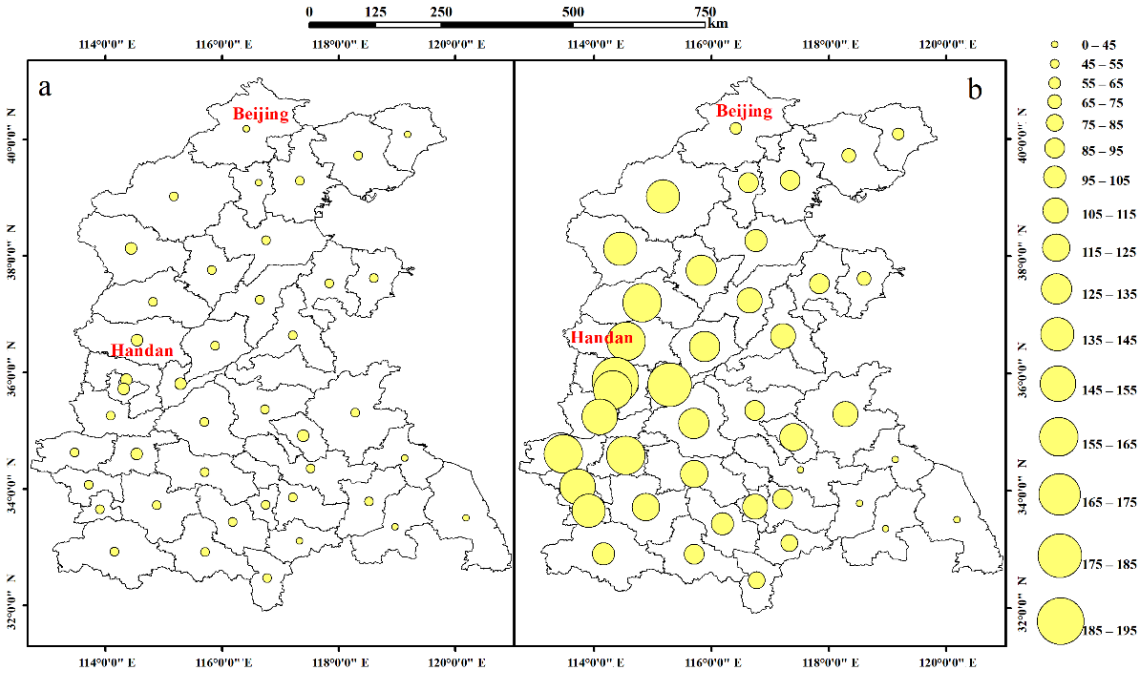

Figure 4. Average $PM_{2.5}$ concentrations in the North China Plain region during (**a**) the COVID-19 lockdown period in 2020, and (**b**) the corresponding period in 2019.

The time series of daily average AQI and concentrations of air pollutants during the COVID-19 period in 2020 and the corresponding period in 2019 are shown in Figure 2, and Figure 5 shows the comparison of the averages of air pollutant concentrations during different stages between 2019 and 2020. As mentioned above, the comparison of air quality data during Stage III of 2019 and 2020 can efficiently reflect the impact of the COVID-19 lockdown (Figures 2 and 5). Compared with during other stages, $PM_{2.5–10}$, $PM_{2.5}$, NO_2, and CO reduced most significantly during Stage III (COVID-19 lockdown) from 2019 to 2020. $PM_{2.5–10}$ showed the largest reduction of 66.6%, followed by NO_2 (58.4%), SO_2 (55.1%), $PM_{2.5}$ (50.1%) and CO (31.3%). However, compared to Stage III in 2019, O_3 increased by 13.9%. These results indicate that the implemented lockdown measures such as quarantine at home and travel restrictions had significant effects on reducing air pollutants, except O_3. Secondary formation played important roles in $PM_{2.5}$ and O_3 formation during the COVID-19 lockdown, especially for the haze periods [11,40]. The reduction in $PM_{2.5}$ and the increase in O_3 emphasized the importance of $PM_{2.5}$ and O_3 synergetic control.

NO_2 reduction and O_3 increase during the COVID-19 lockdown were also reported across most of China, yet the variation extents were different [41–46]. The decrease in NO_2 should mainly be attributed to the significant traffic reductions during the COVID-19 epidemic [41]. The concentration of O_3 is related to that of NO_2 due to the photochemical reactions and titration process. In contrast to NO_2 reduction, O_3 increase was caused by less NO available to react with O_3, as well as less heterogeneous HO_2 radical loss and higher actinic flux (i.e., photochemical formation from precursors such as VOCs) with lower particle concentration [41,44].

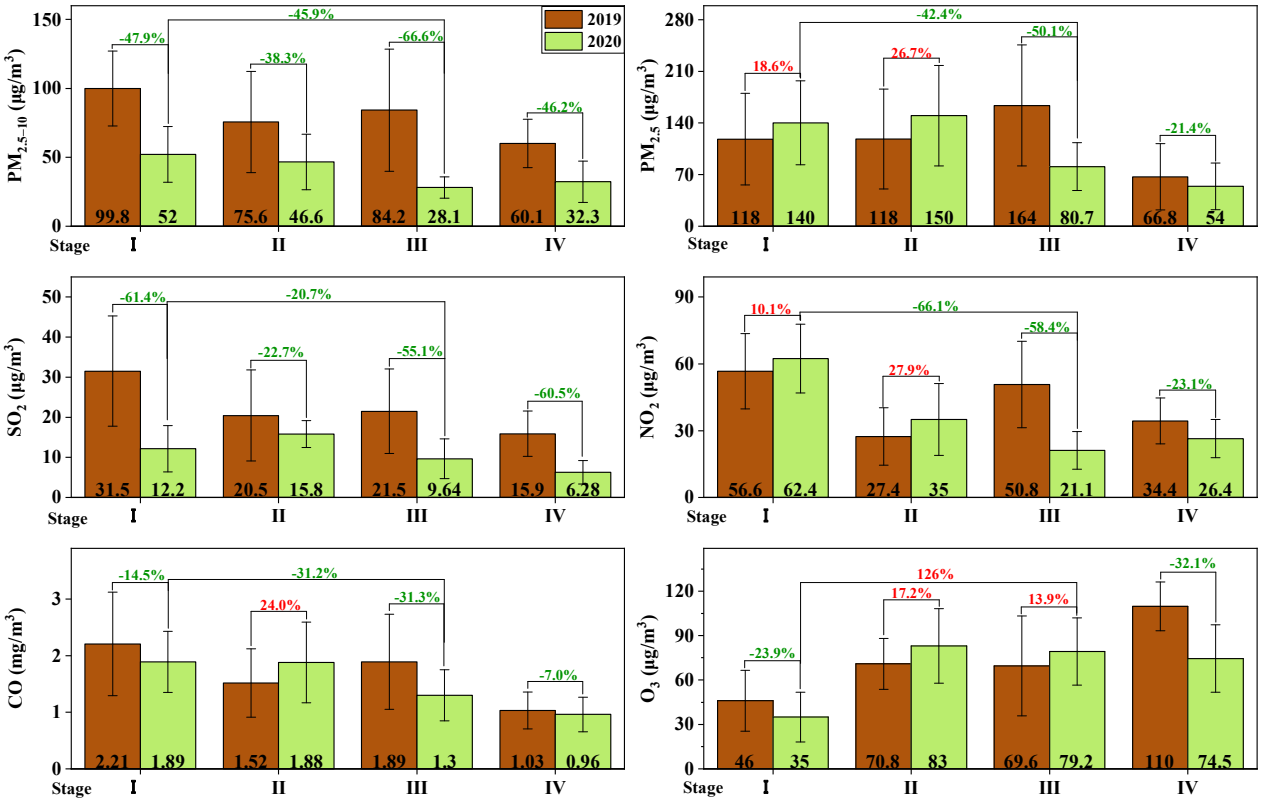

Figure 5. Averages of air pollutant concentrations in Handan during the COVID-19 period in 2020 and the corresponding period in 2019.

It is worth noting that the SO_2 concentration during the COVID-19 period in 2020 was much lower than in 2019, especially in Stage I, III and IV, SO_2 decreased by 61.4%, 55.1% and 60.5% (Figure 5). This result may be related to the total coal consumption control (e.g., the replacement of coal with gas and electricity) implemented in Handan city, which reduced the amount of coal combustion and SO_2 emissions to a certain extent [4,45,46]. During the Chinese New Year period (Stage II), the peak values of $PM_{2.5}$, NO_2 and CO in 2020 were higher than in 2019 (Figure 2), and $PM_{2.5}$, NO_2, CO and O_3 increased by 26.7%, 27.9%, 24.0% and 17.2%, respectively (Figure 5). In contrast, $PM_{2.5–10}$ and SO_2 reduced by 38.3% and 22.7%, respectively; however, the degree was much lower than the other three stages (Figure 5). Hu et al. [47] reported that fireworks during the Chinese New Year period contributed about 59% to $PM_{2.5}$ concentration and 29% to SO_2 in Handan in 2018. These results indicate that the air pollution during the Chinese New Year period was still serious, which was probably caused by the intense primary emissions, e.g., large amounts of fireworks burning in suburban areas [48], and secondary aerosol formation under higher relative humidity (Figure 3). Therefore, banning fireworks during the Chinese New Year period would be important to improve air quality.

Compared with the pre-COVID-19 period in 2020, $PM_{2.5–10}$, $PM_{2.5}$, SO_2, NO_2, and CO decreased by 45.9%, 42.4%, 20.7%, 66.1% and 31.2%, respectively, but O_3 increased by 126% during the COVID-19 lockdown period (Figure 5). NO_2 dropped the most, further indicating that the COVID-19 lockdown significantly reduced traffic emissions. In addition to the comparison between 2019 and 2020, the changes in NO_2 proved that the COVID-19 lockdown indeed reduced NO_2, because the influences of meteorological factors on air quality were secondary during the COVID-19 lockdown period [26]. The significant increase in O_3 might be related to a significant decline in the emission ratio of NO_x and VOCs from anthropogenic emissions due to the strongly VOC-limited conditions in the NCP in winter [39,49]. Under VOC-limited conditions, a reduction in VOCs emission inhibits the O_3 formation, but a reduction in NO_x emission increases the O_3 formation [50].

Liu et al. [51] conducted a comprehensive observation and CMAQ modeling analyses of surface O_3 across China for periods before and during the lockdown and found that the decrease in the emission ratio of NO_x (decreased by 46%) and VOCs (32%) contributed to net O_3 enhancement in North China. To control O_3 pollution in Handan, the synergetic control of NO_x and VOCs is required.

3.2. Distinct Variations in Air Pollutants among the Different Functional Areas

Figure 6 shows the variations in daily air quality at different functional areas in Handan among the four stages during the COVID-19 period. Figure 7 and Table S2 show the changes in air pollutants at different functional areas in Handan during the COVID-19 lockdown period (Stage III) compared with the pre-COVID-19 period (Stage I). $PM_{2.5–10}$, $PM_{2.5}$ and CO significantly decreased in all functional areas (Figures 6 and 7, Table S2), but the reduction degree of air pollutants varied among different functional areas. From Stage I to III, both $PM_{2.5–10}$ (63.7%) and $PM_{2.5}$ (51.5%) showed the largest reduction in the commercial area, $PM_{2.5–10}$ reduced the least in the construction site (31.9%) and the village (32.4%), and the minimum decrease (40.6%) of $PM_{2.5}$ occurred in the scenic area. The different reduction degrees of $PM_{2.5–10}$ and $PM_{2.5}$ were caused by the different sources of particulate pollutants in different functional areas. For instance, dust from construction activities and soil dust in the village contributed more to coarse particles ($PM_{2.5–10}$) [42,52], and the secondary formation of anthropogenic and biogenic precursors contributed more to fine particles in the commercial and scenic areas, respectively.

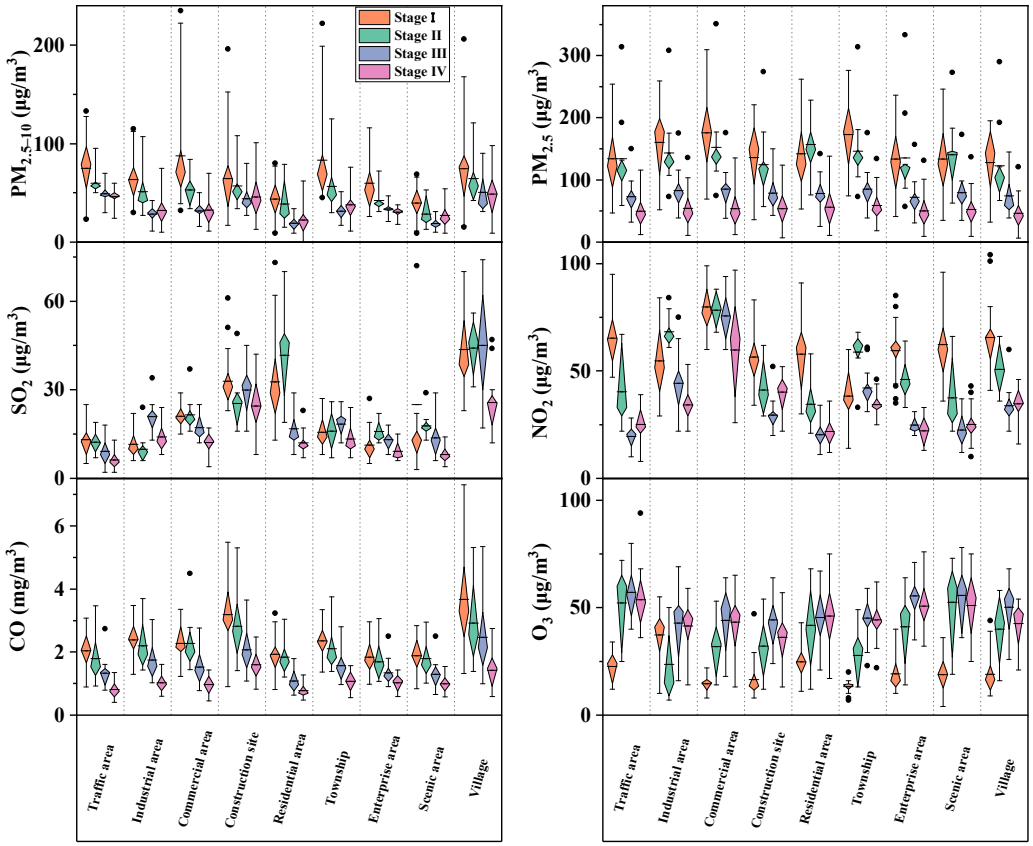

Figure 6. Variations in the concentrations of air pollutants at the different functional areas of Handan during COVID-19 period in 2020. Horizontal lines and dots in each box are the median and mean values, respectively. The 25th and the 75th percentiles are indicated by the lower and the upper boundaries of each box, respectively. The lower and upper whiskers represent the 5th and the 95th percentiles, respectively. The black dots represent outliers.

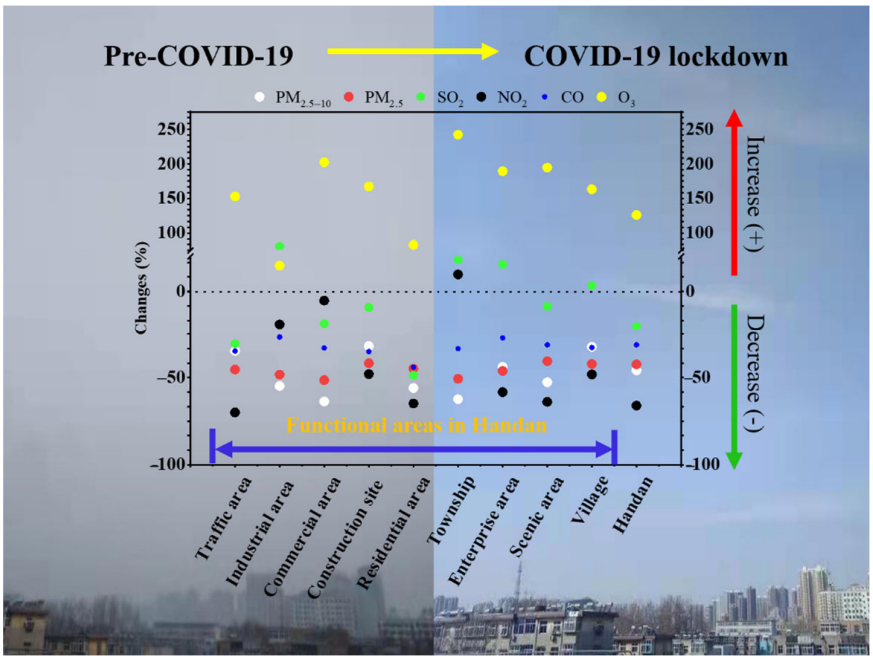

Figure 7. The changes (%) in air pollutants in different functional areas in Handan during the COVID-19 lockdown period (Stage III) compared with the pre-COVID-19 period (Stage I).

SO_2 showed quite different variation trends among different functional areas (Figures 6 and 7, Table S2). SO_2 lowered the most by 48.7% in the residential area, followed by the traffic area (30.5%) and the commercial area (18.6%), while SO_2 reduced by less than 10% or even increased in other functional areas during the COVID-19 lockdown period. The results imply that the restrictions on coal combustion in the urban area (e.g., residential, traffic and commercial areas) were relatively stricter than in other functional areas in Handan. The concentration of SO_2 in the village was higher than other functional areas during the whole observation, although there was a significant reduction during the post-COVID-19 period (Figure 7). Similarly, Yuan et al. [42] reported that compared with the pre-COVID-19 period, the average SO_2 concentrations at an urban site in the megacity Hangzhou, China decreased by 22%, much higher than at urban-industry, and suburban sites (9%) during the COVID-19 lockdown period. Notably, SO_2 showed a great increase of 80.6% in the industrial area, indicating that the major sources of SO_2, e.g., heavy industries, coal-fired power plants and residential heating [26,53,54], were still running during the lockdown. Previous studies also reported that the effects of the COVID-19 control measures on SO_2 were less significant in China [26,54].

NO_2 showed a trend of decrease to different extents in different functional areas, except the township area during the COVID-19 lockdown period. Unsurprisingly, NO_2 in the traffic area plunged dramatically by 70.0% from 65.3 $\mu g/m^3$ (Stage I) to 19.6 $\mu g/m^3$ (Stage III) due to traffic reduction, followed by the residential area (64.9%), scenic area (63.9%) and enterprise area (58.4%), and the least reduction (5.3%) occurred in the commercial area. NO_2 in the township area increased by 9.7%. The changes in NO_2 showed that lockdown measures led to an efficient reduction in emission from vehicles, and the effect was more obvious in the urban area. However, the decrease in the degree of NO_x showed little variations (82–83%) among the urban, urban-industry, and suburban sites in the much more developed city of Hangzhou [42].

CO reduced in all functional areas by 26.8–44.1% during the COVID-19 lockdown period (Figure 6 and Table S2). CO reduced the least (26.8%) in the industrial area and the most in the residential area (44.1%) and the traffic area (34.8%). CO is primarily emitted from industries and vehicles [54,55]. The lowest reduction in the industrial area also related to the running of heavy industries and coal-fired power plants during the lockdown, although CO emitted from vehicles was largely reduced. Figure 7 also showed that the

concentration of CO in the village was higher than other functional areas, followed by the construction site during the whole observation. This was probably because residential heating had to be operational in these areas, and emissions from residential heating was one of the major sources of CO.

In contrast, O_3 showed a significant increase in all functional areas. The largest increase (242.0%) was in the township area, followed by the commercial area (202.3%), the scenic area (194.4%), and the lowest increase (14.7%) in the industrial area. The different increasing degrees in O_3 was probably associated with the different declining emission ratios of NO_x and VOCs in different functional areas [51], for instance, the largest decrease in the emission ratio of NO_x/VOCs in the township area. In addition, surface ozone generation is related to photochemical reactions under solar radiation. The $PM_{2.5}$ and $PM_{2.5–10}$ in the commercial area were reduced more than those in the industrial area nearby. The lower PM would provide more favorable conditions for photochemical generation and the large increase in O_3 in the commercial area. Wu et al. [50] also found that a difference in the increase in O_3 concentration at roadside (64%) and non-roadside (33%) stations during the full lockdown period. Yuan et al. [42] also reported that during the COVID-19 lockdown period, the average O_3 mass concentrations increased differently at the urban, urban-industry and suburban sites by 125%, 114% and 102%, respectively in Hangzhou, China, compared with the pre-COVID-19 period. However, O_3 concentrations in most functional areas in Handan increased by up to about two times (Figure 6 and Table S2), which was much more significant than in Hangzhou during the COVID-19 lockdown period.

Urban stations may experience different weather conditions from semi-urban and rural ones due to urban heat island (UHI), green roofs, anthropogenic heating, etc. These factors also impact the air quality in urban and suburban areas. In this study, we did not consider the influence of these factors on the variation of air pollutants among different functional areas, so it is possible that these conditions could have an impact on the results of our study, which requires further studies in the future.

3.3. Source Identification of Air Pollutants during the COVID-19 Lockdown Period

Although air pollutant emissions were significantly suppressed during the COVID-19 lockdown period in Handan, the levels of O_3 and particle pollution still largely exceeded the WHO air quality guideline values. According to the State of Global Air, air pollution contributed to 6.67 million deaths in 2019 worldwide (https://www.stateofglobalair.org/health/global (accessed on 5 September 2022)). Previous studies have suggested that premature mortality is not only related to locally emitted air pollutants, but also to long-distance transported pollutants [15,56]. Thus, it is necessary to identify the sources of air pollution and make joint efforts to prevent and control air pollution in different regions.

3.3.1. Correlation Analysis

Correlation analysis was applied to identify the sources of air pollution during the COVID-19 period (Table 1). The pollutants with good correlation have similar variation patterns and are likely from the similar emission source, and vice versa [57]. Mobile sources (e.g., vehicles) emit NO_2 and CO [55], while stationary sources (e.g., industrial emissions) emit SO_2 and CO [58]. The correlation between NO_2 and CO was generally more significant than that between SO_2 and CO in Handan (Table 1), implying that CO was more related to mobile sources. There were significant positive correlations between NO_2 and $PM_{2.5–10}$, $PM_{2.5}$, SO_2 and CO during the pre-COVID-19 period, indicating that vehicle exhausts were a major pollution source. During the COVID-19 lockdown period, the correlation coefficients between $PM_{2.5}$, and SO_2, CO increased, but the correlation coefficients between $PM_{2.5}$ and NO_2 decreased. This result verifies that stationary sources (e.g., industrial emissions) made a significant contribution to $PM_{2.5}$ during this period in Handan. The large heavy industries, coal-fired power plants, and household cooking and heating continued to run, although some small private industries were closed in Handan during the COVID-19 lockdown period [44,54]. The relatively slight reduction in SO_2 and

CO concentrations further supports this argument (Figure 5). Compared with Stage III in 2019, NO_2 showed a more significant correlation with $PM_{2.5–10}$, $PM_{2.5}$, SO_2 and CO during the COVID-19 lockdown period, probably because NO_2 was also emitted from sources similar to $PM_{2.5–10}$, $PM_{2.5}$, SO_2 and CO, such as industrial sources, when the traffic source of NO_2 reduced.

Table 1. The correlation between air pollutants during the COVID-19 period in 2020 and the corresponding period in 2019.

2019	$PM_{2.5–10}$	$PM_{2.5}$	SO_2	NO_2	CO	2020	$PM_{2.5–10}$	$PM_{2.5}$	SO_2	NO_2	CO
Stage I						Stage I					
$PM_{2.5}$	0.834 **					$PM_{2.5}$	0.592 **				
SO_2	0.019	−0.009				SO_2	0.564 **	0.199			
NO_2	0.592 **	0.627 **	0.688 **			NO_2	0.628 **	0.799 **	0.581 **		
CO	0.611 **	0.772 **	0.405	0.797 **		CO	0.493 *	0.804 **	−0.108	0.541 *	
O_3	−0.681 **	−0.628 **	−0.251	−0.725 **	−0.526 *	O_3	−0.240	−0.511*	−0.22	−0.480 *	−0.443
Stage II						Stage II					
$PM_{2.5}$	0.879 **					$PM_{2.5}$	0.798 **				
SO_2	0.780 **	0.671 *				SO_2	0.261	−0.236			
NO_2	0.711 *	0.874 **	0.654 *			NO_2	0.956 **	0.647 *	0.411		
CO	0.795 **	0.927 **	0.621 *	0.898 **		CO	0.707 *	0.820 **	−0.064	0.673 *	
O_3	0.367	0.13	0.701 *	0.134	0.22	O_3	−0.833 **	−0.482	−0.379	−0.844 **	−0.257
Stage III						Stage III					
$PM_{2.5}$	0.943 **					$PM_{2.5}$	0.757 **				
SO_2	0.008	−0.012				SO_2	0.435	0.344			
NO_2	0.616 *	0.564 *	0.649 *			NO_2	0.640 *	0.709 **	0.812 **		
CO	0.719 **	0.701 **	0.335	0.780 **		CO	0.742 **	0.926 **	0.603 *	0.875 **	
O_3	−0.305	−0.238	0.594 *	0.211	0.296	O_3	0.243	−0.032	0.655 *	0.468	0.175
Stage IV						Stage IV					
$PM_{2.5}$	0.712 **					$PM_{2.5}$	0.413				
SO_2	−0.020	0.158				SO_2	0.381	−0.001			
NO_2	0.217	0.445	0.808 **			NO_2	0.287	0.725 **	0.276		
CO	0.199	0.534 *	0.854 **	0.835 **		CO	0.242	0.839 **	0.052	0.750 **	
O_3	0.416	0.580 *	0.148	0.338	0.464	O_3	0.339	−0.353	0.527 *	−0.342	−0.246

Note: ** Correlation is significant at the 0.01 level (2-tailed); * Correlation is significant at the 0.05 level (two-tailed).

During the COVID-19 lockdown and post-COVID-19 periods, O_3 exhibited an insignificant correlation ($p > 0.05$) with other air pollutants (except for SO_2), while it was negatively correlated with other air pollutants during the pre-COVID-19 and Chinese New Year periods in 2020. These results suggest that the traffic control would be effective to reduce particulate pollution but would not prevent a rise in O_3, as mentioned above [41,43].

3.3.2. Diagnostic Ratio Analysis

The WHO suggested that the ratio of $PM_{2.5}/PM_{10}$ is 0.65 for developed countries and 0.5 for developing countries in the absence of a locally measured ratio [59], demonstrating that the reduction in $PM_{2.5}$ is crucial for controlling atmospheric particulate pollution. The $PM_{2.5}/PM_{10}$ ratio is useful in reflecting the contribution of anthropogenic emissions to particulate pollutants [60]. From Stage I to III, there were no obvious changes (~0.71) in $PM_{2.5}/PM_{10}$ (Figure 8), indicating that fine particles dominated particulate pollution due to intense anthropogenic emissions in Handan; the pollution sources of fine and coarse ($PM_{2.5–10}$) particles are similar during these periods, as evidenced by the significant correlation (Table 1).

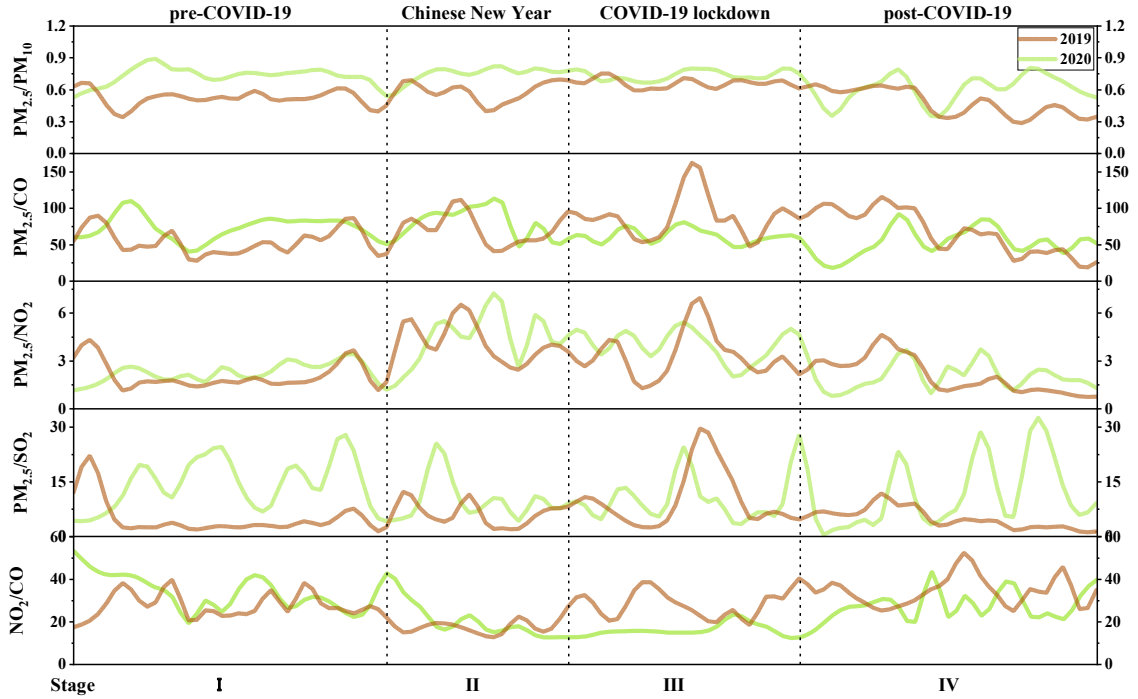

Figure 8. The ratios of air pollutants in Handan during the COVID-19 period in 2020 and the corresponding period in 2019.

The $PM_{2.5}$/CO ratio is used as a good indicator of primary combustion sources [61]. A higher $PM_{2.5}$/CO ratio suggests a more important contribution of secondary formation to $PM_{2.5}$ than primary emission. The $PM_{2.5}$/CO ratio decreased from 72.7 during Stage I to 62.0 during Stage III, and $PM_{2.5}/SO_2$ also slightly decreased from 13.9 to 10.6 (Figure 8), but the correlations between $PM_{2.5}$ and CO, SO_2 became more significant (Table 1). These results suggest that stationary sources such as industrial emissions played an important role during the COVID-19 lockdown period. In contrast, $PM_{2.5}/NO_2$ increased from 2.2 to 4.0 (Figure 8) and their correlation became weaker (Table 1), while NO_2/CO reduced largely from 34.5 to 16.1. These results imply that the COVID-19 lockdown measures led to a much more significant reduction in NO_2 and CO from mobile source emissions in Handan [55].

Compared with the corresponding period in 2019, the ratios of $PM_{2.5}$ to PM_{10}, CO, NO_2 and SO_2 were larger during the pre-COVID-19 period, and particularly, $PM_{2.5}/SO_2$ increased most significantly. These results suggest that the coal substitution policy implemented in Hebei province since 2017 achieved a remarkable effect, leading to a decrease in SO_2 emissions from 2019 to 2010 (Figures 4 and 5). Compared with 2019, the ratios of $PM_{2.5}/PM_{10}$ and $PM_{2.5}/SO_2$ were slightly or significantly higher in 2020 during Stage II, as mentioned above, which may mainly be caused by enhanced $PM_{2.5}$ due to fireworks emissions and/or secondary formation.

3.3.3. Backward Trajectory Clustering and Potential Source Analysis

In order to further understand the possible factors affecting air pollution in Handan city during the COVID-19 period, the backward trajectories of air masses were calculated and clustered (Figure 9).

During the pre-COVID-19 period (Figure 9a), the majority of air masses (except Cluster 5) transported slowly from southern Hebei province and surrounding areas, indicating a regional or local contribution to air pollution in Handan. During the Chinese New Year period (Figure 9c), the air masses also mainly originated from southern Hebei (Cluster 2, 4, 5) or the surrounding northern Henan province (Cluster 1) and moved slowly. A minor fraction of the air masses came northeasterly across Shandong Province from Bohai Sea (16.7%, Cluster 3, 6). During the COVID-19 lockdown period (Figure 9e), the air masses

mainly came westerly from Shanxi Province (Cluster 2, 6) and easterly or northeasterly from Hebei province (Cluster 1, 5), and a part of them originated from the central southern Henan province (Cluster 4). During the post-COVID-19 period (Figure 9g), the air masses originating from northern Henan province (Category 3) accounted for the most (27.0%), and long-distance transported air masses from Inner Mongolia (Cluster 1) and Mongolia (Cluster 4) accounted for 17.3% and 15.5%, respectively, followed by those from southern Hebei, Shanxi and Shaanxi provinces.

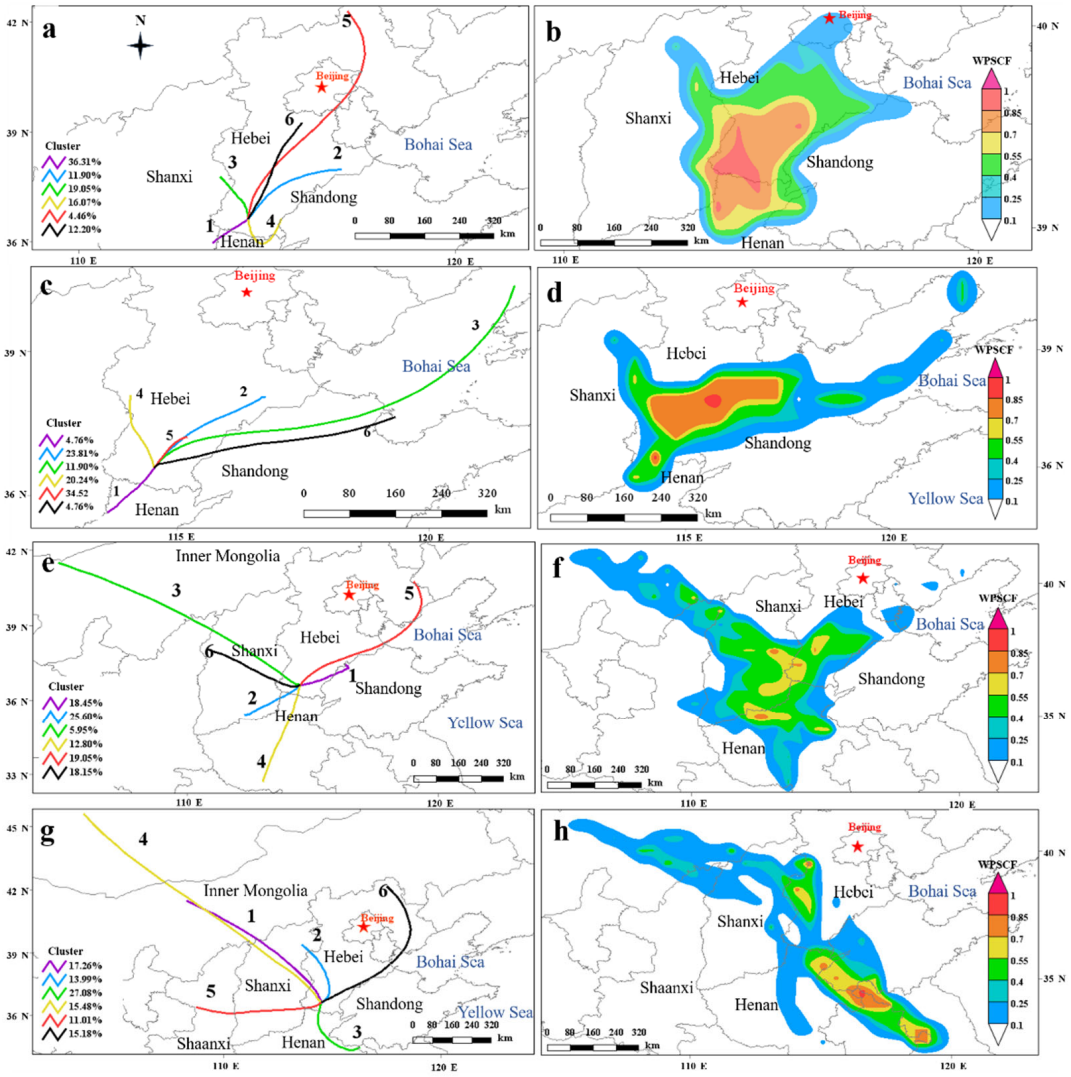

Figure 9. Cluster analysis of air mass backward trajectories (**a**,**c**,**e**,**g**) and potential source regions of $PM_{2.5}$ (**b**,**d**,**f**,**h**) in Handan during the COVID-19 period in 2020. (**a**,**b**) Pre-COVID-19 period, (**c**,**d**) Chinese New Year period, (**e**,**f**) COVID-19 lockdown period, and (**g**,**h**) post-COVID-19 period.

Previous studies have researched the interregional transport of air pollution. For example, Chang et al. (2019) indicated that, although local $PM_{2.5}$ emissions were dominant in all 13 cities within the BTH area, regional transport from Shandong and Henan Provinces contributed as much as 12.9% of $PM_{2.5}$ emissions [62]. Zhang et al. (2017) reported that large quantities of air pollutants (primary $PM_{2.5}$) were transported to the BTH region from Shandong, Jiangsu, Anhui, and Henan provinces via the southerly wind, accounting for 11.6%, 9.2%, 6.7%, 11.8% of BTH, respectively [63]. Moreover, Chang et al. (2022) found that the inter-transport contributions of black carbon increased extensively above the atmospheric boundary layer of the Yangtze River Delta under stable weather conditions [64].

Therefore, it is necessary to further explore the interregional transport of air pollution to provide suggestions for pollution prevention measures during the COVID-19 period.

To investigate the spatial distribution of air pollution sources during the COVID-19 period in Handan city, the primary pollutant $PM_{2.5}$ was selected for a potential source analysis (Figure 9). The areas with high WPSCF values (more than 0.55) were mainly distributed in the surrounding areas of Handan in Hebei province and the surrounding provinces of Shanxi, Henan and Shandong during the pre-COVID-19 period (Figure 9b). During the Chinese New Year period, the main source areas of $PM_{2.5}$ were concentrated in southern Hebei province (Figure 9d). In these two periods, local emissions or regional transported pollutants made a major contribution to air pollution in Handan. During the COVID-19 lockdown period (Figure 9f) and post-COVID-19 period (Figure 9h), the areas with high WPSCF values (more than 0.55) largely shrunk, indicating that the $PM_{2.5}$ pollution in all surrounding regions of Handan eased.

In addition, the contribution of long-distance or inter-regional transport to heavy $PM_{2.5}$ pollution weakened significantly. This was likely a benefit of the COVID-19 lockdown measures across China, implying that the implementation of the joint prevention and control of atmospheric pollution policy is effective to improve air quality.

4. Conclusions

By comparing with the corresponding period in 2019 and comparing with different functional areas of Handan, we analyzed the air quality changes related to the lockdown during the COVID-19 period. Compared with 2019, $PM_{2.5–10}$, $PM_{2.5}$, NO_2 and CO exhibited the largest reduction during the COVID-19 lockdown period (Stage III) in 2020. NO_2 decreased the most by 58.4%, followed by $PM_{2.5–10}$ (66.6%), SO_2 (55.1%), $PM_{2.5}$ (50.1%) and CO (31.3%), whereas O_3 increased by 13.9% during Stage III from 2019 to 2020. These results imply that the lockdown measures had significant effects on reducing air pollutants, except O_3. The opposite variations in $PM_{2.5}$ and O_3 emphasized the importance of $PM_{2.5}$ and O_3 synergetic control due to their secondary formation from precursors. Similarly, from the pre-COVID-19 period to the COVID-19 lockdown period in 2020, the reductions in $PM_{2.5–10}$, $PM_{2.5}$, SO_2, NO_2 and CO were significant, especially NO_2 (66.1%), but O_3 increased by 126%. The significant increase in O_3 might result from the decline in the emission ratio of NO_x and VOCs from anthropogenic emissions under strongly VOC-limited conditions in the NCP. To control O_3 pollution in Handan, the synergetic control of NO_x and VOCs is required.

Among different functional areas in Handan, air pollutants showed distinct variation degrees from the pre-COVID-19 period to the COVID-19 lockdown period. Both $PM_{2.5–10}$ (63.7%) and $PM_{2.5}$ (51.5%) showed the largest reduction in the commercial area. NO_2 showed the largest reduction (70%) in the traffic area. SO_2 lowered the most by 48.7% in the residential area but increased greatly by 80.6% in the industrial area. O_3 pollution increased in all functional areas to different extents (14.7–242%). These results reflect that the sources of air pollutants in different functional areas are different, so it is necessary to formulate air pollution control measures according to functional areas.

The correlation analysis and ratio analysis among different air pollutants verified that stationary sources (e.g., industrial emissions) made a significant contribution to $PM_{2.5}$ during the COVID-19 lockdown period in Handan. In addition, COVID-19 lockdown measures led to a much more significant reduction in NO_2 and CO from mobile source emissions. However, a control on traffic emissions would be effective to reduce particulate pollution but would not prevent a rise in O_3 in Handan. The potential source contribution function analysis indicated that the $PM_{2.5}$ pollution in all surrounding regions of Handan eased, and the contribution of long-distance or inter-regional transport to heavy $PM_{2.5}$ pollution weakened significantly during the lockdown period. The natural experiment during the COVID-19 period demonstrated that the implementation of the joint prevention and control of atmospheric pollution policy is effective to improve air quality.

Supplementary Materials: The following supporting information can be downloaded at: https://www.mdpi.com/article/10.3390/su141811531/s1, Table S1: "Information of the monitoring stations in the nine different functional areas in Handan"; Table S2: "The changes (%) of air pollutants at different functional areas in Handan during COVID-19 lockdown period (Stage III) compared with the pre-COVID-19 period (Stage I)".

Author Contributions: H.N. and W.H. designed the study. C.Z. performed the data analysis. C.Z., W.H. and H.N. prepared the paper, with contributions from all co-authors (T.H., C.W., S.H., L.F.O.S., N.G., X.B. and J.F.). All authors have read and agreed to the published version of the manuscript.

Funding: This work was supported by the National Natural Science Foundation of China (41807305, 41977183); Hebei Provincial Natural Science Foundation (D2021402004); the National Key Program of the Cause and Control of Severe Air Pollution (DQGG202110); and the Technology Innovation Center Fund of Hebei Province for the Detection and Treatment of VOCs in Chemical Industry (ZXJJ20210402).

Institutional Review Board Statement: Not applicable.

Informed Consent Statement: Not applicable.

Data Availability Statement: No online data availability.

Conflicts of Interest: The authors declare no conflict of interest.

References

1. Bu, X.; Xie, Z.; Liu, J.; Wei, L.; Wang, X.; Chen, M.; Ren, H. Global $PM_{2.5}$ attributable health burden from 1990 to 2017: Estimates from the Global Burden of disease study 2017. *Environ. Res.* **2021**, *197*, 111123. [CrossRef] [PubMed]
2. Cheng, J.; Su, J.; Cui, T.; Li, X.; Dong, X.; Sun, F.; Yang, Y.; Tong, D.; Zheng, Y.; Li, Y.; et al. Dominant role of emission reduction in $PM_{2.5}$ air quality improvement in Beijing during 2013–2017: A model-based decomposition analysis. *Atmos. Chem. Phys.* **2019**, *19*, 6125–6146. [CrossRef]
3. Yan, D.; Lei, Y.; Shi, Y.; Zhu, Q.; Li, L.; Zhang, Z. Evolution of the spatiotemporal pattern of $PM_{2.5}$ concentrations in China-a case study from the Beijing-Tianjin-Hebei region. *Atmos. Environ.* **2018**, *183*, 225–233. [CrossRef]
4. Zeng, J.J.; Liu, T.; Feiock, R.; Li, F. The impacts of China's provincial energy policies on major air pollutants: A spatial econometric analysis. *Energy Policy* **2019**, *132*, 392–403. [CrossRef]
5. Xue, F.; Niu, H.; Hu, S.; Wu, C.; Zhang, C.; Gao, N.; Ren, X.; Li, S.; Hu, W.; Wang, J.; et al. Seasonal variations and source apportionment of carbonaceous aerosol in $PM_{2.5}$ from a coal mining city in the North China Plain. *Energy Explor. Exploit.* **2021**, *40*, 834–851. [CrossRef]
6. Song, X.; Jia, J.; Wu, F.; Niu, H.; Ma, Q.; Guo, B.; Shao, L.; Zhang, D. Local emissions and secondary pollutants cause severe $PM_{2.5}$ elevation in urban air at the south edge of the North China Plain: Results from winter haze of 2017–2018 at a mega city. *Sci. Total Environ.* **2021**, *802*, 149630. [CrossRef]
7. Chen, S.; Yang, J.; Yang, W.; Wang, C.; Bärnighausen, T. COVID-19 control in China during mass population movements at New Year. *Lancet* **2020**, *395*, 764–766. [CrossRef]
8. Wang, Y.; Wen, Y.; Wang, Y.; Zhang, S.; Zhang, K.M.; Zheng, H.; Xing, J.; Wu, Y.; Hao, J. Four-month changes in air quality during and after the COVID-19 lockdown in six megacities in China. *Environ. Sci. Technol. Lett.* **2020**, *7*, 802–808. [CrossRef]
9. Tian, H.; Liu, Y.; Li, Y.; Wu, C.H.; Chen, B.; Kraemer, M.U.G.; Li, B.; Cai, J.; Xu, B.; Yang, Q.; et al. An investigation of transmission control measures during the first 50 days of the COVID-19 epidemic in China. *Science* **2020**, *368*, 638–642. [CrossRef]
10. Wang, C.; Horby, P.W.; Hayden, F.G.; Gao, G.F. A novel coronavirus outbreak of global health concern. *Lancet* **2020**, *395*, 470–473. [CrossRef]
11. Huang, X.; Ding, A.; Gao, J.; Zheng, B.; Zhou, D.; Qi, X.; Tang, R.; Wang, J.; Ren, C.; Nie, W.; et al. Enhanced secondary pollution offset reduction of primary emissions during COVID-19 lockdown in China. *Natl. Sci. Rev.* **2021**, *8*, nwaa137. [CrossRef]
12. Zambrano-Monserrate, M.A.; Ruano, M.A.; Sanchez-Alcalde, L. Indirect effects of COVID-19 on the environment. *Sci. Total Environ.* **2020**, *728*, 138813. [CrossRef]
13. Shi, X.; Brasseur, G.P. The response in air quality to the reduction of Chinese economic activities during the COVID-19 outbreak. *Geophys. Res. Lett.* **2020**, *47*, e2020GL088070. [CrossRef]
14. Adam, M.G.; Tran, P.T.M.; Balasubramanian, R. Air quality changes in cities during the COVID-19 lockdown: A critical review. *Atmos. Res.* **2021**, *264*, 105823. [CrossRef]
15. Lelieveld, J.; Evans, J.S.; Fnais, M.; Giannadaki, D.; Pozzer, A. The contribution of outdoor air pollution sources to premature mortality on a global scale. *Nature* **2015**, *525*, 367–371. [CrossRef]
16. Rahman, M.M.; Paul, K.C.; Hossain, M.A.; Ali, G.G.M.N.; Rahman, M.S.; Thill, J.C. Machine learning on the COVID-19 pandemic, human mobility and air quality: A review. *IEEE Access* **2021**, *9*, 72420–72450. [CrossRef]

17. Gamelas, C.; Abecasis, L.; Canha, N.; Almeida, S.M. The Impact of COVID-19 Confinement Measures on the Air Quality in an Urban-Industrial Area of Portugal. *Atmosphere* **2021**, *12*, 1097. [CrossRef]
18. Ropkins, K.; Tate, J.E. Early observations on the impact of the COVID-19 lockdown on air quality trends across the UK. *Sci. Total Environ.* **2021**, *754*, 142374. [CrossRef]
19. Wang, Q.; Li, S. Nonlinear impact of COVID-19 on pollutions—Evidence from Wuhan, New York, Milan, Madrid, Bandra, London, Tokyo and Mexico City. *Sustain. Cities Soc.* **2021**, *65*, 102629. [CrossRef]
20. Kroll, J.H.; Heald, C.L.; Cappa, C.D.; Farmer, D.K.; Fry, J.L.; Murphy, J.G.; Steiner, A.L. The complex chemical effects of COVID-19 shutdowns on air quality. *Nat. Chem.* **2020**, *12*, 777–779. [CrossRef]
21. He, G.; Pan, Y.; Tanaka, T. The short-term impacts of COVID-19 lockdown on urban air pollution in China. *Nat. Sustain.* **2020**, *3*, 1005–1011. [CrossRef]
22. Lian, X.; Huang, J.; Huang, R.; Liu, C.; Wang, L.; Zhang, T. Impact of city lockdown on the air quality of COVID-19-hit of Wuhan city. *Sci. Total Environ.* **2020**, *742*, 140556. [CrossRef]
23. Hu, X.; Liu, Q.; Fu, Q.; Xu, H.; Shen, Y.; Liu, D.; Wang, Y.; Jia, H.; Cheng, J. A high-resolution typical pollution source emission inventory and pollution source changes during the COVID-19 lockdown in a megacity, China. *Environ. Sci. Pollut. Res.* **2021**, *28*, 45344–45352. [CrossRef]
24. Zhang, K.; de Leeuw, G.; Yang, Z.; Chen, X.; Jiao, J. The impacts of the COVID-19 lockdown on air quality in the Guanzhong Basin, China. *Remote Sens.* **2020**, *12*, 3042. [CrossRef]
25. Wang, H.; Tan, Y.; Zhang, L.; Shen, L.; Zhao, T.; Dai, Q.; Guan, T.; Ke, Y.; Li, X. Characteristics of air quality in different climatic zones of China during the COVID-19 lockdown. *Atmos. Pollut. Res.* **2021**, *12*, 101247. [CrossRef]
26. Pei, Z.; Han, G.; Ma, X.; Su, H.; Gong, W. Response of major air pollutants to COVID-19 lockdowns in China. *Sci. Total Environ.* **2020**, *743*, 140879. [CrossRef]
27. Niu, H.; Wu, Z.; Xue, F.; Liu, Z.; Hu, W.; Wang, J.; Fan, J.; Lu, Y. Seasonal variations and risk assessment of heavy metals in PM from Handan, China. *World J. Eng.* **2021**, *18*, 886–897. [CrossRef]
28. Polissar, A.V.; Hopke, P.K.; Paatero, P.; Kaufmann, Y.J.; Hall, D.K.; Bodhaine, B.A.; Dutton, E.G.; Harris, J.M. The aerosol at Barrow, Alaska: Long-term trends and source locations. *Atmos. Environ.* **1999**, *33*, 2441–2458. [CrossRef]
29. Abbott, M.L.; Lin, C.J.; Martian, P.; Einerson, J.J. Atmospheric mercury near Salmon Falls Creek Reservoir in southern Idaho. *Appl. Geochem.* **2008**, *23*, 438–453. [CrossRef]
30. Xu, X.; Akhtar, U. Identification of potential regional sources of atmospheric total gaseous mercury in Windsor, Ontario, Canada using hybrid receptor modeling. *Atmos. Chem. Phys.* **2010**, *10*, 7073–7083. [CrossRef]
31. Cheng, M.D.; Lin, C.J. Receptor modeling for smoke of 1998 biomass burning in Central America. *J. Geophys. Res.* **2001**, *106*, 22871–22886. [CrossRef]
32. Qiao, Z.; Wu, F.; Xu, X.; Yang, J.; Liu, L. Mechanism of spatiotemporal air quality response to meteorological parameters: A national-scale analysis in China. *Sustainability* **2019**, *11*, 3957. [CrossRef]
33. Pateraki, S.; Asimakopoulos, D.N.; Flocas, H.A.; Maggos, T.; Vasilakos, C. The role of meteorology on different sized aerosol fractions (PM_{10}, $PM_{2.5}$, $PM_{2.5\text{-}10}$). *Sci. Total Environ.* **2012**, *419*, 124–135. [CrossRef] [PubMed]
34. Wang, Y.; Liu, C.; Wang, Q.; Qin, Q.; Ren, H.; Cao, J. Impacts of natural and socioeconomic factors on $PM_{2.5}$ from 2014 to 2017. *J. Environ. Manag.* **2021**, *284*, 112071. [CrossRef]
35. Hu, W.; Hu, M.; Hu, W.W.; Zheng, J.; Chen, C.; Wu, Y.; Guo, S. Seasonal variations in high time-resolved chemical compositions, sources, and evolution of atmospheric submicron aerosols in the megacity Beijing. *Atmos. Chem. Phys.* **2017**, *17*, 9979–10000. [CrossRef]
36. Liu, F.; Zhang, G.; Lian, X.; Fu, Y.; Lin, Q.; Yang, Y.; Bi, X.; Wang, X.; Peng, P.; Sheng, G. Influence of meteorological parameters and oxidizing capacity on characteristics of airborne particulate amines in an urban area of the Pearl River Delta, China. *Environ. Res.* **2022**, *212*, 113212. [CrossRef]
37. Zhang, Q.; Zheng, Y.; Tong, D.; Shao, M.; Wang, S.; Zhang, Y.; Xu, X.; Wang, J.; He, H.; Liu, W.; et al. Drivers of improved $PM_{2.5}$ air quality in China from 2013 to 2017. *Proc. Natl. Acad. Sci. USA* **2019**, *116*, 24463–24469. [CrossRef]
38. Zhang, X.; Xu, X.; Ding, Y.; Liu, Y.; Zhang, H.; Wang, Y.; Zhong, J. The impact of meteorological changes from 2013 to 2017 on $PM_{2.5}$ mass reduction in key regions in China. *Sci. China Earth Sci.* **2019**, *62*, 1885–1902. [CrossRef]
39. Xing, J.; Li, S.; Jiang, Y.; Wang, S.; Ding, D.; Dong, Z.; Zhu, Y.; Hao, J. Quantifying the emission changes and associated air quality impacts during the COVID-19 pandemic on the North China Plain: A response modeling study. *Atmos. Chem. Phys.* **2020**, *20*, 14347–14359. [CrossRef]
40. Li, R.; Zhao, Y.; Fu, H.; Chen, J.; Peng, M.; Wang, C. Substantial changes in gaseous pollutants and chemical compositions in fine particles in the North China Plain during the COVID-19 lockdown period: Anthropogenic vs meteorological influences. *Atmos. Chem. Phys.* **2021**, *21*, 8677–8692. [CrossRef]
41. Chu, B.; Zhang, S.; Liu, J.; Ma, Q.; He, H. Significant concurrent decrease in $PM_{2.5}$ and NO_2 concentrations in China during COVID-19 epidemic. *J. Environ. Sci.* **2021**, *99*, 346–353. [CrossRef]
42. Yuan, Q.; Qi, B.; Hu, D.; Wang, J.; Zhang, J.; Yang, H.; Zhang, S.; Liu, L.; Xu, L.; Li, W. Spatiotemporal variations and reduction of air pollutants during the COVID-19 pandemic in a megacity of Yangtze River Delta in China. *Sci. Total Environ.* **2021**, *751*, 141820. [CrossRef]
43. Ding, J.; Dai, Q.; Li, Y.; Han, S.; Zhang, Y.; Feng, Y. Impact of meteorological condition changes on air quality and particulate chemical composition during the COVID-19 lockdown. *J. Environ. Sci.* **2021**, *109*, 45–56. [CrossRef]

44. Liu, L.; Zhang, J.; Du, R.; Teng, X.; Hu, R.; Yuan, Q.; Tang, S.; Ren, C.; Huang, X.; Xu, L.; et al. Chemistry of atmospheric fine particles during the COVID-19 pandemic in a megacity of eastern China. *Geophys. Res. Lett.* **2021**, *48*, 2020GL091611. [CrossRef]
45. Xu, M.; Qin, Z.; Zhang, S. Integrated assessment of cleaning air policy in China: A case study for Beijing-Tianjin-Hebei region. *J. Clean. Prod.* **2021**, *296*, 126596. [CrossRef]
46. Wu, Z.; Hu, T.; Hu, W.; Shao, L.; Sun, Y.; Xue, F.; Niu, H. Evolution in physico-chemical properties of fine particles emitted from residential coal combustion based on chamber experiment. *Gondwana Res.* **2022**, *110*, 252–263. [CrossRef]
47. Hu, B.; Duan, J.; Liu, S.; Hu, J.; Zhang, M.; Kang, P.; Wang, C. Evaluation of the Effect of Fireworks Prohibition in the Beijing-Tianjin-Hebei and Surrounding Areas during the Spring Festival of 2018. *Res. Environ. Sci.* **2019**, *32*, 203–211.
48. Xian, T.; Li, Z.; Wei, J. Changes in air pollution following the COVID-19 epidemic in Northern China: The role of meteorology. *Front. Environ. Sci.* **2021**, *9*, 654651. [CrossRef]
49. He, Z.; Liu, P.; Zhao, X.; He, X.; Liu, J.; Mu, Y. Responses of surface O_3 and $PM_{2.5}$ trends to changes of anthropogenic emissions in summer over Beijing during 2014-2019: A study based on multiple linear regression and WRF-Chem. *Sci. Total Environ.* **2021**, *807*, 150792. [CrossRef]
50. Wu, C.L.; Wang, H.W.; Cai, W.J.; He, H.D.; Ni, A.N.; Peng, Z.R. Impact of the COVID-19 lockdown on roadside traffic-related air pollution in Shanghai, China. *Build. Environ.* **2021**, *194*, 107718. [CrossRef]
51. Liu, Y.; Wang, T.; Stavrakou, T.; Elguindi, N.; Doumbia, T.; Granier, C.; Bouarar, I.; Gaubert, B.; Brasseur, G.P. Diverse response of surface ozone to COVID-19 lockdown in China. *Sci. Total Environ.* **2021**, *789*, 147739. [CrossRef] [PubMed]
52. Guo, X.; Wu, H.; Chen, D.; Ye, Z.; Shen, Y.; Liu, J.; Cheng, S. Estimation and prediction of pollutant emissions from agricultural and construction diesel machinery in the Beijing-Tianjin-Hebei (BTH) region, China. *Environ. Pollut.* **2020**, *260*, 113973. [CrossRef]
53. Zhang, L.; An, J.; Liu, M.; Li, Z.; Liu, Y.; Tao, L.; Liu, X.; Zhang, F.; Zheng, D.; Gao, Q.; et al. Spatiotemporal variations and influencing factors of $PM_{2.5}$ concentrations in Beijing, China. *Environ. Pollut.* **2020**, *262*, 114276. [CrossRef]
54. Zheng, X.; Guo, B.; He, J.; Chen, S.X. Effects of corona virus disease-19 control measures on air quality in North China. *Environmetrics* **2021**, *32*, e2673. [CrossRef]
55. Sokhi, R.S.; Singh, V.; Querol, X.; Finardi, S.; Targino, A.C.; Andrade, M.F.; Pavlovic, R.; Garland, R.M.; Massague, J.; Kong, S.; et al. A global observational analysis to understand changes in air quality during exceptionally low anthropogenic emission conditions. *Environ. Int.* **2021**, *157*, 106818. [CrossRef]
56. Hassler, B.; McDonald, B.C.; Frost, G.J.; Borbon, A.; Carslaw, D.C.; Civerolo, K.; Granier, C.; Monks, P.S.; Monks, S.; Parrish, D.D.; et al. Analysis of long-term observations of NOx and CO in megacities and application to constraining emissions inventories. *Geophys. Res. Lett.* **2016**, *43*, 9920–9930. [CrossRef]
57. Bai, Y.; Wang, Z.; Xie, F.; Cen, L.; Xie, Z.; Zhou, X.; He, J.; Lu, C. Changes in stoichiometric characteristics of ambient air pollutants pre-to post-COVID-19 in China. *Environ. Res.* **2022**, *209*, 112806. [CrossRef]
58. Zhang, Q.; Jiang, X.; Tong, D.; Davis, S.J.; Zhao, H.; Geng, G.; Feng, T.; Zheng, B.; Lu, Z.; Streets, D.G.; et al. Transboundary health impacts of transported global air pollution and international trade. *Nature* **2017**, *543*, 705–709. [CrossRef]
59. Ostro, B.; World Health Organization/Occupational Environmental Health Team. *Outdoor Air Pollution: Assessing the Environmental Burden of Disease at National and Local Levels*; World Health Organization: Geneva, Switzerland, 2004.
60. Zha, H.; Wang, R.; Feng, X.; An, C.; Qian, J. Spatial characteristics of the $PM_{2.5}/PM_{10}$ ratio and its indicative significance regarding air pollution in Hebei Province, China. *Environ. Monit. Assess.* **2021**, *193*, 486. [CrossRef]
61. Fu, S.; Guo, M.; Fan, L.; Deng, Q.; Han, D.; Wei, Y.; Luo, J.; Qin, G.; Cheng, J. Ozone pollution mitigation in guangxi (south China) driven by meteorology and anthropogenic emissions during the COVID-19 lockdown. *Environ. Pollut.* **2021**, *272*, 115927. [CrossRef]
62. Chang, X.; Wang, S.; Zhao, B.; Xing, J.; Liu, X.; Wei, L.; Song, Y.; Wu, W.; Cai, S.; Zheng, H.; et al. Contributions of inter-city and regional transport to $PM_{2.5}$ concentrations in the Beijing-Tianjin-Hebei region and its implications on regional joint air pollution control. *Sci. Total Environ.* **2019**, *660*, 1191–1200. [CrossRef] [PubMed]
63. Zhang, Y.; Zhu, B.; Gao, J.; Kang, H.; Yang, P.; Wang, L.; Zhang, J. The Source Apportionment of Primary $PM_{2.5}$ in an Aerosol Pollution Event over Beijing-Tianjin-Hebei Region using WRF-Chem, China. *Aerosol Air Qual. Res.* **2017**, *17*, 2966–2980. [CrossRef]
64. Cheng, Y.; Zhu, B.; Wang, L.; Lu, W.; Kang, H.; Gao, J. Source apportionments of black carbon induced by local and regional transport in the atmospheric boundary layer of the Yangtze River Delta under stable weather conditions. *Sci. Total Environ.* **2022**, *840*, 156517. [CrossRef] [PubMed]